

## Infinite-randomness critical point in the itinerant quantum antiferromagnet

Rastko Sknepnek<sup>1,2</sup> and Thomas Voja<sup>1</sup><sup>1</sup>Department of Physics, University of Missouri-Rolla, Rolla, MO 65409<sup>2</sup>Institut für Physik, Technische Universität, D-09107 Chemnitz, Germany

(Dated: April 14, 2024)

We study the quantum phase transition in the three-dimensional disordered itinerant antiferromagnet by Monte-Carlo simulations of the order-parameter field theory. We find strong evidence for the transition being controlled by an infinite-randomness fixed point: The dynamical scaling is activated, i.e., the logarithm of the energy scales like a power of the length, implying a dynamical exponent of infinity. The probability distribution of the energy gaps is very broad and becomes broader with increasing system size, even on a logarithmic scale.

Phase transitions in systems with quenched disorder are an important topic in statistical physics. The critical behavior of systems with quenched disorder can be divided into three classes, according to the behavior of the disorder under coarse graining. In the first class, disorder decreases under coarse graining, and the system becomes asymptotically homogeneous at large length scales. Technically, this means the disorder is renormalization group irrelevant, and the transition is controlled by a "clean" fixed point (FP). According to the Harris criterion [1] this happens if the clean FP fulfills  $2 > d$ , where  $2$  is the correlation length critical exponent and  $d$  is the spatial dimensionality. In this first class the macroscopic observables are self-averaging at the critical point, i.e., the relative width of their probability distributions goes to zero in the thermodynamic limit [2, 3].

In the second class, the system remains inhomogeneous at all length scales with the relative strength of the inhomogeneities approaching a finite value for large length scales. These transitions are controlled by renormalization group FPs with finite disorder. Macroscopic observables are not self-averaging, the relative width of their probability distributions approaches a size-independent constant [2, 3]. Examples of critical points in the second class include the dilute three-dimensional Ising model, classical spin glasses, and various other thermal critical points in disordered systems.

The third possibility occurs when the relative magnitude of the inhomogeneities increases without limit under coarse graining. The corresponding renormalization group FPs are called infinite-randomness FPs. At these FPs the probability distributions of macroscopic variables become very broad (on a logarithmic scale) with the width increasing with system size. Consequently, averages will be often dominated by rare events, e.g., spatial regions with atypical disorder configurations. Infinite-randomness critical points have mainly been found for quantum phase transitions since the disorder, being perfectly correlated in (imaginary) time direction, has a stronger effect for quantum phase transitions than for thermal ones. Examples include the random transverse-field Ising and Potts chains [4, 5, 6] and the

two-dimensional transverse-field Ising model [7, 8].

A natural question is, how general is the occurrence of infinite-randomness FPs in disordered quantum systems. One prototypical and particularly controversial transition is the antiferromagnetic quantum phase transition of disordered itinerant electrons in three dimensions which is believed to be important, e.g., for a variety of heavy-fermion materials [9]. It has been investigated by various methods but no definite results could be achieved. In the absence of disorder this transition is controlled by a Gaussian FP with mean-field static critical exponents and a dynamical exponent of  $z = 2$  [10]. According to the Harris criterion [1] this clean FP is unstable with respect to disorder, and the transition, if any, must be in class two or three of the above classification. Within the conventional perturbative renormalization group [11] one finds a finite-disorder FP suggesting that the transition belongs to class two. However, the renormalization group flow diagram, Fig. 1, shows that a system with weak initial (bare) disorder is taken to large disorder at intermediate stages of the renormalization before spiraling into the FP. This casts serious doubts on the validity of the perturbative approach. Indeed, by taking into account the effects of rare regions it was later shown [12] that the conventional FP is unstable and the renormalization group flow is towards large disorder in all of the physical parameter space. The ultimate fate of the transition, however, could not be determined within this approach. Possible scenarios included a complete destruction of the transition, a conventional FP (i.e., class two) inaccessible by perturbative methods, or an infinite-randomness FP.

In this Letter we contribute to the solution of this puzzle by reporting results from large-scale computer simulations of the antiferromagnetic quantum phase transition of disordered itinerant electrons in three dimensions with uniaxial (Ising) symmetry. We find strong evidence for a sharp phase transition which is controlled by an infinite-randomness FP similar to those in the random transverse-field Ising models [4, 5, 6, 7, 8]. Specifically, we find that the probability distribution of the order parameter susceptibility (the inverse energy gap) becomes broader with increasing system size, even on a logarithmic

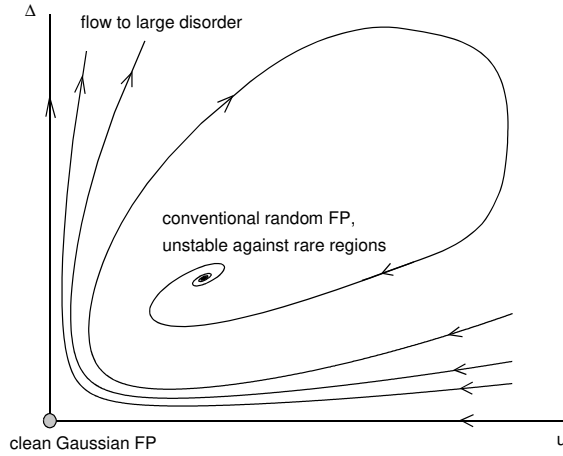


FIG. 1: Schematic of the perturbative renormalization group flow.  $\Delta$  is the disorder strength and  $u$  is a measure of the quantum fluctuations

mic scale. The entire distribution scales with  $\ln L$  with  $\beta = 0.39$ . This implies a dynamical exponent of  $z = 1$ . The average gap and the average order parameter susceptibility follow stretched exponentials with different powers. In the rest of the paper we outline our calculations and discuss the results in detail.

The simulation of the full disordered interacting electron problem is numerically very expensive. Consequently, the system sizes are so severely restricted that an investigation of the critical behavior is essentially impossible in three dimensions. Rather than simulating the full problem we have therefore performed simulations of the Landau-Ginzburg-Wilson (LGW) theory of the phase transition which contains only the long-wave-length, low-frequency fluctuations of the order parameter. This approach is valid close to the transition as long as the (bare) disorder is weak so that local phenomena like the formation of localized moments do not play an important role.

The LGW theory of the antiferromagnetic quantum phase transition of itinerant electrons in  $d$  dimensions is equivalent to a classical ferromagnet in  $d + 2$  dimensions with the disorder being uncorrelated in the  $d$  "space-like" dimensions but completely correlated in the two "time-like" dimensions [11, 13]. In the following we concentrate on three spatial dimensions and uniaxial symmetry. For an efficient simulation we map the field theory to a lattice model. The quenched disorder is introduced via site dilution in the "space-like" dimensions, i.e., the impurities are two-dimensional holes in the  $d$ -dimensional lattice. The classical model Hamiltonian reads

$$H = \sum_{\langle \mathbf{r}, \mathbf{r}' \rangle} S(\mathbf{r}; \tau) S(\mathbf{r}'; \tau) : \quad (1)$$

Here  $\mathbf{r} = (x, y, z)$  and  $\tau = (\tau_1, \tau_2)$  are the "space-like" and "time-like" coordinates of lattice sites, respectively;

and the sum runs over all pairs of nearest neighbors.  $S(\mathbf{r}; \tau) = \pm 1$  is an Ising spin, and  $\tau$  is a quenched random variable with values 0 and 1 and an average of  $\langle \tau \rangle = p$  (the symbol  $\langle \cdot \rangle$  denotes the disorder average). All the results in this Letter are for  $p = 0.8$  while the percolation threshold for three-dimensional site percolation is  $p = 0.31$ . The rather weak disorder allows us to observe the crossover from the clean Gaussian FP to the infinite-randomness FP using the system size as a renormalization cutoff. In the model Hamiltonian the transition is tuned by changing the classical temperature  $T_{cl}$  which is different from the physical temperature of the quantum system; the latter is encoded in the length of the system in time-direction.

For the Monte-Carlo simulations we have employed the Wolff cluster algorithm [14]. We have studied systems with linear sizes up to  $L = 29$  in space direction and also  $L = 29$  in time direction (the largest system having 20 million sites). We found that no more than 200 sweeps were required for equilibration. Between 1000 and 5000 disorder configurations were considered, depending on system size with at least 1000 measurement sweeps per disorder configuration.

To get an overview over the behavior of the system we have computed the average Binder parameter

$$[g] = \frac{1}{3} \frac{\langle M^4 \rangle}{\langle M^2 \rangle^2} : \quad (2)$$

Here  $M$  is the magnetization and  $\langle \cdot \rangle$  denotes the thermodynamic average for a single sample.  $[g]$  has the expected finite-size scaling form

$$[g] = g(tL^{1/\nu}; L^{-\nu}) \text{ conventional FP}, \quad (3)$$

$$[g] = g(tL^{1/\nu}; \ln L = L) \text{ infinite-randomness FP} \quad (4)$$

Here  $t = (T_{cl} - T_c)/T_c$  is the distance from the critical point. The dynamical scaling is of power-law type at a conventional FP but activated at an infinite-randomness FP [4]. As a result of its scale dimension being zero,  $[g]$  is easily analyzed: provided  $L$  is scaled appropriately with  $t$ , a point in parameter space where  $[g]$  is independent of the system size corresponds to a renormalization group FP. In principle, both  $\nu$  and  $z$  (or  $\beta$ ) can be determined from the finite-size scaling of  $[g]$  [7].

In Fig. 2 we show the Binder parameter  $[g]$  as a function of the classical temperature  $T_{cl}$  for different system sizes  $L = L_0 \dots L_{max}$ . For small sizes,  $L = 7 \dots 10$ , the curves cross at  $T_{cl} = 7.88$ . However, for larger sizes this crossing point becomes unstable and a new crossing emerges at  $T_{cl} = 7.96$ . A comparison with the flow diagram in Fig. 1 suggests that the former crossing point corresponds to the clean Gaussian FP. (A system with small bare disorder first approaches the Gaussian FP under renormalization before it goes to large disorder.) To check this hypothesis we have performed a series of calculations at

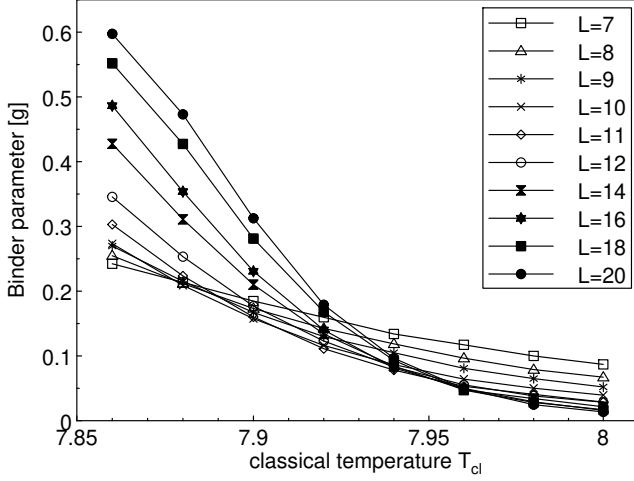


FIG. 2: Average Binder parameter  $[g]$  as a function of classical temperature  $T_{cl}$  for different system sizes.

$T_{cl} = 7.88$ , independently varying  $L$  and  $L_c$ . The maximum of  $[g]$  as a function of  $L$  occurs at  $L = L_c$  as expected at the Gaussian FP. A standard finite-size scaling analysis based on (3) yields exponents of  $\nu = 0.55$  and  $z = 1.0$ . Since the range of available sizes at this unstable crossing is very limited the agreement with the expected values  $\nu_c = 0.5$  and  $z_c = 1$  is surprisingly good [15]. We conclude that the crossing point at  $T_{cl} = 7.88$  indeed corresponds to the clean Gaussian FP.

We now turn to the crossing point at  $T_{cl} = 7.96$  which we attribute to the critical FP of the phase transition. We have again performed a series of calculations independently varying  $L$  and  $L_c$ . However, the dependence of  $[g]$  on  $L$  for fixed  $L_c$  turned out to be very weak. (At  $T_{cl} = 7.96$  and  $L = 18$ ,  $[g]$  remained constant at  $g_c = 0.048$  within our statistical error of about 6% for all  $L$  between 12 and 29.) This can be explained by the fact that the critical value,  $g_c = 0.048$ , is very small, which corresponds to weak average correlations. This tends to reduce the influence of the boundary conditions and thus the sample shape [16]. Consequently, finite-size scaling of  $[g]$  is not an efficient method to study the dynamical scaling of this critical point. For all further calculations we have therefore used samples with  $L = L_c$ . Fig. 3 shows the average Binder parameter  $[g]$  for systems with  $L = 12$  in the vicinity of the critical point at  $T_{cl} = 7.96$ . The inset shows that the data scale reasonably well with a correlation length exponent of  $\nu = 1.0$ .

In order to further analyze the critical behavior we now consider the probability distribution of the order parameter susceptibility  $\chi$ , i.e., the inverse energy gap. At a conventional finite-disorder FP the distribution of  $\chi$  should be size-independent [2, 3]. In Fig. 4 we show this distribution at the critical point,  $T_{cl} = 7.96$ , for different system sizes. Clearly the distribution becomes

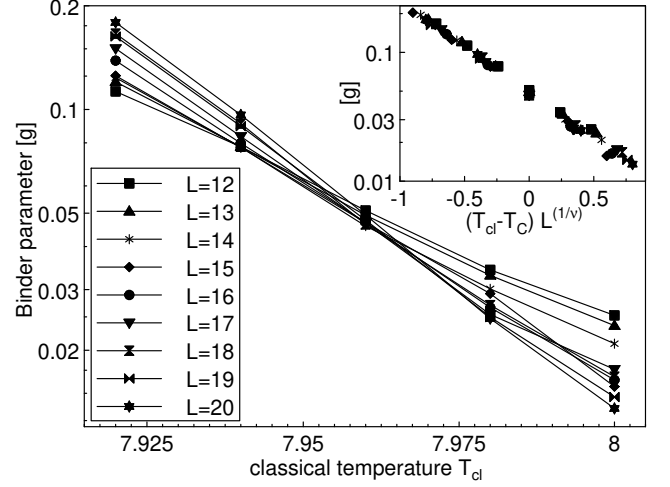


FIG. 3: Log. plot of the Binder parameter  $[g]$  close to the critical point. At  $T = 7.96$  the standard deviation is about one symbol size. Inset: Finite-size scaling plot using  $\nu = 1$ .

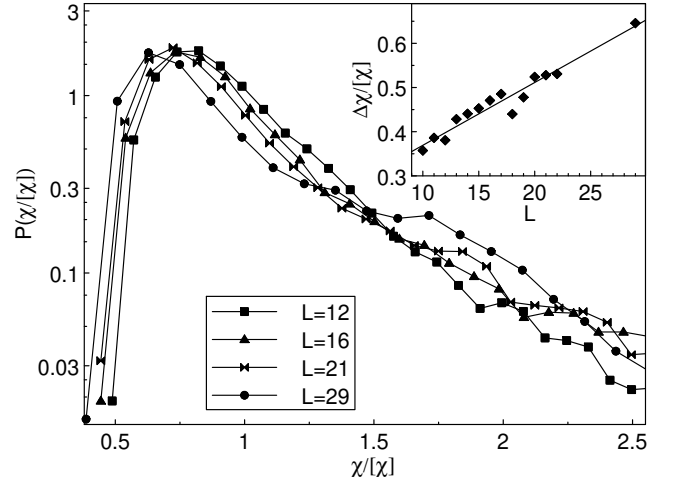


FIG. 4: Distribution of the order parameter susceptibility  $\chi = [g]$  at the critical point  $T_{cl} = 7.96$  for different sizes (at least 2300 disorder configurations were used for the distributions). Inset: Dependence of  $\Delta\chi/[chi]$  on  $L$ .

broader with increasing  $L$ . This can also be seen from the inset which shows the relative widths of the distribution as a function of system size. This suggests that the phase transition is controlled by an infinite-randomness FP rather than a conventional one.

At an infinite-randomness FP we expect activated scaling [4],  $\ln \chi \sim L^\nu$ . In Fig. 5 we show a corresponding scaling plot of the distribution of  $\ln \chi$ . The distribution scales with an exponent of  $\nu = 0.39$ . The inset shows the size-dependence of the logarithm of the typical susceptibility,  $\ln \chi_{typ} = [\ln \chi]$ . The solid line is a power-law fit,  $\ln \chi_{typ} \sim L^\nu$ , which gives the same exponent of  $\nu = 0.39$ .

We now consider the average susceptibility  $[g]$  and the

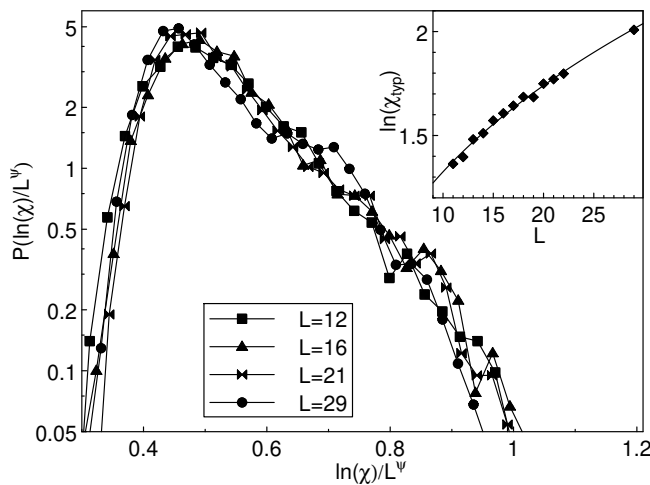


FIG. 5: Distribution of  $x = \ln(L)$  at  $T_{cl} = 7.96$  using  $\beta = 0.39$ . Inset: Dependence of  $\ln(x_{typ})$  on  $L$ . The solid line is a power law fit with the same exponent  $\beta = 0.39$ .

average gap  $[L=]$ . Since for large  $L$  the distribution of  $\ln$  becomes very broad,  $[L=]$  will be dominated by the large- $(\ln)$  tail of the distribution. For large  $x = \ln(L)$  the distribution in Fig. 5 approximately falls as  $e^{-x^2}$ . For large  $L$  the integral for  $[L=]$  can be treated in saddle point approximation giving an asymptotic size dependence of  $\ln[L=] \sim L^2$ . The average order parameter susceptibility increases faster with system size than the typical one. Analogously, the average energy gap  $[L=]$  will be dominated by the small- $(\ln)$  tail of the distribution. However, the accuracy of our data is not sufficient to determine the functional form of this tail. For system sizes  $L = 12$  to  $29$  the susceptibility distribution is not sufficiently broad yet for the above saddle-point argument to apply. In this size range we numerically obtain the effective relations  $\ln[L=] \sim L^{0.45}$  and  $\ln[L=] \sim L^{0.37}$ . While the exponent of  $\ln[L=]$  is larger than  $\beta$ , it is much smaller than the asymptotic value of  $2 - \beta = 0.78$ .

In summary, we have found strong evidence for an infinite-randomness FP at the antiferromagnetic quantum phase transition of disordered itinerant electrons in three dimensions. This FP has properties similar to those found in the random transverse-field Ising model in one and two dimensions. We conclude with two remarks. First, the systems we were able to simulate are rather modest in linear size because the effective dimensionality of the LGW theory is very high. Therefore all quantitative results for critical exponents should be understood as effective rather than asymptotic values. Second, the results obtained here are for the case of uniaxial symmetry. The qualitative features of the perturbative flow diagram in Fig. 1 including the runaway flow to large disorder, are the same for Ising, XY or Heisenberg symmetry. This suggests that the transition is controlled by

an infinite-randomness FP for the XY and Heisenberg cases, too. However, in Ref. [8] it was found that the random-singlet FP in localized XY or Heisenberg antiferromagnets [17, 18, 19], another example of an infinite-randomness FP, becomes unstable for  $d > 1$ , suggesting that a continuous order parameter symmetry tends to weaken infinite-randomness FPs. It thus remains unclear whether the antiferromagnetic quantum phase transition of disordered itinerant electrons with XY or Heisenberg symmetry is controlled by any of the known types of FPs or whether it belongs to a new class.

We gratefully acknowledge discussions with Dietrich Belitz, Ted Kirkpatrick and Rajesh Narayanan. This work was supported in part by the German Research Foundation under grant nos. Vo659/2, Vo659/3 and SFB 393/C2 and by the University of Missouri Research Board. The bulk of the calculations was performed on the CLIC parallel supercomputer of Chemnitz University of Technology, using a total of about 6000 CPU days.

- 
- [1] A. B. Harris, J. Phys. C 7, 1671 (1974)
  - [2] A. Aharony and A. B. Harris, Phys. Rev. Lett. 77, 3700 (1996)
  - [3] S. W. Ismael and E. Domany, Phys. Rev. Lett. 81, 22 (1998)
  - [4] D. S. Fisher, Phys. Rev. 69, 534 (1992); Phys. Rev. B 51, 6411 (1995)
  - [5] T. Senthil and S. N. Majumdar, Phys. Rev. Lett. 76, 3001 (1996)
  - [6] A. P. Young and H. Rieger, Phys. Rev. B 53, 8486 (1996)
  - [7] C. Pich, A. P. Young, H. Rieger, and N. Kawashima, Phys. Rev. Lett. 81, 5916 (1998); C. Pich and A. P. Young, cond-mat/9802108
  - [8] O. Motrunich, S.-C. Ma, D. A. Huse, and D. S. Fisher, Phys. Rev. B 61, 1160 (2000)
  - [9] M. C. de Andrade et al., Phys. Rev. Lett. 81, 5620 (1998)
  - [10] J. Hertz, Phys. Rev. B 14, 1165 (1976)
  - [11] T. R. Kirkpatrick and D. Belitz, Phys. Rev. Lett. 76, 2571 (1996); 78, 1197 (1997)
  - [12] R. Narayanan, T. Vojta, D. Belitz, and T. R. Kirkpatrick, Phys. Rev. Lett. 82, 5132 (1999); Phys. Rev. B 60, 10150 (1999)
  - [13] D. Boyanovsky and J. Cardy, Phys. Rev. B 26, 154 (1982)
  - [14] U. Wol, Phys. Rev. Lett. 62, 361 (1989)
  - [15] Note that the value of the dynamical exponent  $z$  in the original quantum problem is twice as large as that of our classical lattice model since we have mapped the time direction onto two additional space dimensions.
  - [16] This is in marked contrast to simulations of the random transverse-field Ising models [7] where the maximum  $[g]$  at the critical point is approximately 0.55 in 1D and 0.35 in 2D. Correspondingly, the dependence of  $[g]$  on the shape is stronger and the dynamical exponent can be determined from a finite-size scaling analysis of  $[g]$ .
  - [17] S. K. Ma, C. Dasgupta, and C.-K. Hu, Phys. Rev. Lett. 43, 1434 (1979)
  - [18] R. N. Bhatt and P. A. Lee, Phys. Rev. Lett. 48, 344 (1982)
  - [19] D. S. Fisher, Phys. Rev. B 50, 3799 (1994)